

Regularities of orbit sizes of valence nucleons

A. Moalem

Department of Physics, Ben-Gurion University, Beer-Sheva, Israel

(Received 18 January 1982)

Precision measurements of orbit sizes indicate that the root mean square radius decreases almost linearly as the particle separation energy increases at the rate $\partial r/\partial \epsilon = -0.08$ fm MeV⁻¹.

[NUCLEAR STRUCTURE Systematics of orbit sizes, implication for
mean field theories.]

Considerable interest has been devoted recently to determining the root mean square (rms) radii of single particle orbits within nuclei.¹⁻¹⁶ Apart from being a vital input for a significant interpretation of the cross section for a variety of nuclear processes, the rms radii of individual shells provide a stringent test for current mean field theories and may serve to critically evaluate the microscopic structure which underlies the calculated charge and matter distributions. While mean field theories appear to account in detail for the observed distributions,¹⁷ there are significant discrepancies between the measured rms radii of valence orbits and the calculated ones. In particular, magnetic electron scattering¹⁻⁵ and single particle transfer reactions⁷⁻¹⁶ lead to radii which are consistently smaller than those predicted by density-dependent Hartree-Fock (DDHF) and density-dependent Hartree-Fock-Bogoliubov (DDHFB) calculations. More recently, it was indicated by Dubach⁶ that the inclusion of exchange currents, which were not included in the analyses of Refs. 1-5, would increase the rms radii from magnetic electron scattering, and hence improve the agreement with the results from mean field theories. It is the purpose of the present work to show that precision measurements of orbit radii argue for simple regularities which are not usually reproduced by the common Hartree-Fock (HF) calculations. This deficiency appears to be inherent to HF theories and in particular to the DDHF and DDHFB predictions which are quoted in Ref. 6.

We examine orbit radii from three different sources: (i) single particle transfer reactions,⁷⁻¹⁶ (ii) magnetic electron scattering,¹⁻⁶ and (iii) particle knockout reactions.¹⁸ These results are listed in Table I and are displayed graphically versus the particle separation energy in Fig. 1. The methods of analyses and the reliability of the results from

each of these processes are discussed in detail in Refs. 1, 11, and 18, but some basic features deserve mention here. First, the reaction cross sections calculated in distorted wave theories depend strongly on the rms radius of the particle bound state wave function $\phi_{nlj}(r)$. Commonly, ϕ is calculated in a Woods-Saxon (WS) potential whose depth and geometrical parameters are adjusted to reproduce the particle separation energy and the measured cross section. The actual functional form of the potential is not critical, since quite large changes in the potential parameters have little effect on the radii extracted.¹¹ Second, the extraction of radii from transfer reaction data is feasible only if the reaction normalization (\mathcal{N}) and the spectroscopic factors (C^2S) of the transition involved are known accurately. The large body of spectroscopic factors that are available in the literature is not very useful for this purpose, since the strong dependence of C^2S on the orbit size is generally disregarded. To obtain reliable spectroscopic factors, one may apply a normalization procedure based on spin dependent sum rule (SDSR) analyses.¹¹

It should be emphasized that SDSR analyses may provide two normalization constants (n^+ for stripping and n^- for pickup) only when applied for nuclei of nonzero spin. The results listed in Table I are mostly those obtained from such analyses. Many other reaction studies apply a single normalization constant for both stripping and pickup reactions, and hence should be considered with extra care. For example, in Refs. 7-10, the spectroscopic factors are derived from renormalizing the total transfer sums to the total sum rule limit. Although the total sum can be set equal to the sum rule limit, each of the partial sums for stripping and pickup may depart significantly from the correct values. With these criticisms in mind, we included in Fig. 1

TABLE I. Root mean square radii of point single particle orbits.

$(Nlj)_N$	System	BE (MeV)	G_{lj}^2 ^a	r_N (fm)	Ref.	
$(2s_{1/2})_\pi$	²⁸ Si-p	13.8	knockout	3.33 ^d	18	
	³⁵ Cl-p	9.680	0.98±0.03	3.54 ±0.10	16	
	³⁷ Cl-p	11.709	1.00±0.03	3.50 ±0.10	16	
	⁴⁰ Ca-p	11.2	knockout	3.53 ^d	18	
	⁵⁸ Ni-p	9.3	knockout	3.73 ^d	18	
$(2s_{1/2})_v$	³⁵ Cl-n	15.216	0.10±0.02	3.35 ±0.10	16	
	³⁵ Cl+n	6.623	0.14±0.02	3.99 ±0.10	16	
$(1f_{7/2})_v$	⁴⁵ Sc-n	11.319	0.38±0.015	3.832±0.04	13	
	⁴⁵ Sc+n	9.276	0.55±0.018	4.033±0.04	13	
	⁴⁹ Ti-n		8.146	m.e.s. ^b	4.011±0.04	2
				m.e.s.	4.121±0.05 ^c	6
$(1f_{7/2})_\pi$	⁵¹ V-n	10.944	1.10±0.10	3.90 ±0.06	15	
	⁵¹ V-p	8.057	0.75±0.04	3.97 ±0.04	15	
				m.e.s. ^b	4.006±0.04	3
				m.e.s.	4.092±0.04 ^c	6
	⁵¹ V+p	10.501	0.48±0.03	3.92 ±0.06	15	
⁵⁹ Co-p	7.375	m.e.s.	4.036±0.09	3		
			m.e.s.	4.126±0.10 ^c	6	
$(2p_{1/2})_\pi$	⁹¹ Zr-p	8.709	0.49±0.02	4.42 ±0.06	12	
	⁹¹ Zr+p	5.849	0.41±0.02	4.66 ±0.06	12	
$(2p_{3/2})_v$	⁴⁸ Ti+n	9.526		4.42 ±0.07	7	
$(1g_{9/2})_v$	⁸⁷ Sr-n	7.437	m.e.s.	4.655±0.04	4	
			m.e.s.	4.885±0.04 ^c	6	
$(1g_{9/2})_\pi$	⁹¹ Zr-p	9.389	0.40±0.03	4.58 ±0.06	12	
	⁹¹ Zr+p	5.849	2.55±0.18	4.87 ±0.06	12	
	⁹³ Nb-p	6.031	m.e.s.	4.834±0.035	4	
			m.e.s.	4.988±0.09 ^c	6	
$(2d_{5/2})_v$	⁹¹ Zr-n	7.194	1.09±0.08	5.02 ±0.15	12	
	⁹¹ Zr+n	8.640	0.30±0.03	4.93 ±0.15	12	

^a G_{lj}^2 stands for the usual C^2S and $(2J_f+1)/(2J_i+1)C^2S$ experimental quantities from pickup and stripping, respectively.

^bFrom the study of the magnetic component of elastic electron scattering (m.e.s.).

^cFrom m.e.s. with exchange currents included.

^dValues calculated with the potentials listed in Table III of Ref. 18. No errors are reported. Quoting Mougey *et al.*, the radii can be determined to better than 5%.

the radii of the $(3s_{1/2})_v$ orbit in the tin isotopes¹⁰ and the $(2p_{3/2})_v$ orbit in ⁴⁹Ti (Ref. 7).

We turn now to radii as obtained from the study of magnetic electron scattering. In Table I we list the values of Refs. 1-5 and the results of Dubach⁶ from more recent analyses of the same data. Dubach⁶ presents the results from several fits to the data both excluding and including exchange currents. The WS radii generally agree with the results from the previous analysis.¹⁻⁵ The radii of

the $1g_{9/2}$ orbit in ⁸⁷Sr and ⁹³Nb, along with the ones for the ⁹¹Zr+N systems, determine a linear curve which appears to be characteristic for the data points of other orbits as well (solid lines of Fig. 1). The fact that knockout reactions, single particle transfers, and magnetic electron scattering determine the same line should not be disregarded. When exchange currents are included, there is an increase in the rms radii typically of the order of 2-3%. These corrections are a bit too large for a

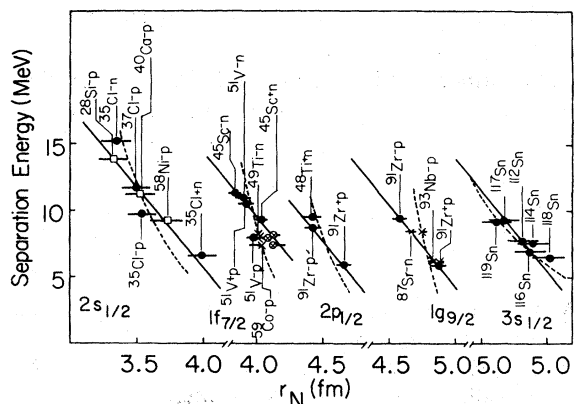


FIG. 1. Radii of point nucleon orbits vs particle separation energy. —□—, from $(e, e'p)$; —●—, transfer reaction data; —×—, magnetic electron scattering with WS fits; and —⊗—, magnetic electron scattering with exchange currents included. The solid lines have no physical significance and were drawn to guide the eye only. The dashed curves represent the predictions for a particle bound in a WS potential (with diffusivity $a=0.65$ fm and a spin orbit term $\lambda=25$ MeV).

$1g_{9/2}$ nucleon in ^{87}Sr and ^{93}Nb and impose some difficulties in interpreting the results from transfer reactions. As indicated in Ref. 14, a value of 4.885 fm for the rms radius of the $(1g_{9/2})_v$ orbit in ^{87}Sr would imply that the total neutron transfer strength is only $\sim 50\%$ of the sum rule limit. This is a particularly unreasonable result for neutron transfers to the $N=50$ closed neutron shell ^{88}Sr nucleus. The two versions of analysis agree, however, that the rms radius of a $1g_{9/2}$ proton in ^{93}Nb is significantly larger than the one of a neutron in ^{87}Sr .

In summary, the results displayed in Table I and Fig. 1 argue for the following observations: (i) The rms radius decreases as the particle separation energy increases, and, within an energy range of several MeV (5–10 MeV), the dependence of the rms radius on the separation energy is nearly linear. (ii) For the $2s_{1/2}$, $1f_{7/2}$, $2p_{1/2}$, $1g_{9/2}$, and $3s_{1/2}$ orbits the rms radius changes with nearly the same rate $\partial r/\partial \epsilon = -0.08$ fm MeV $^{-1}$ (solid lines of Fig. 1). The only two data points for the $(2d_{5/2})_v$ orbit fall also on such a “universal” line but obviously more data is needed to make a firm statement for this orbit. (iii) For nuclei having comparable masses, the rms radius of a specific orbit (nlj) is determined almost solely by the binding energy. The dependence on the mass number A is weak and certainly does not follow the simple $A^{1/3}$ law. This behavior is

different from the A dependence of the optical potential radius as obtained from nucleon scattering. As indicated previously, these observations are significant since they are based on different sources of information.

While observation (i) can be explained from quite general considerations, it is rather difficult to justify a common rate $\partial r/\partial \epsilon$ for all orbits. By virtue of the weak dependence on A , one may simulate the dependence on ϵ in terms of a particle bound in a WS well. The dashed curves of Fig. 1 correspond to a WS well with fixed geometrical parameters. It should be indicated that the shape of these curves is not affected when nonlocality corrections are included or otherwise when the geometrical parameters and the spin orbit term (λ) are modified within a reasonable range. The calculated WS curves agree in general with experiment for $2s_{1/2}$, $3s_{1/2}$, and $2p_{1/2}$ orbits, but depart in the cases of the $1f_{7/2}$ and $1g_{9/2}$ orbits. Based on the data presented above it is perhaps premature to determine the exact functional dependence of r on ϵ . Nonetheless, the data do show that the rate $\partial r/\partial \epsilon$ is negative and nearly the same for all orbits within the energy range 5–10 MeV. This property is not usually reproduced by mean field theories. Clearly, there is some variation in the different HF calculations, but it seems quite general that $\partial r/\partial \epsilon$ is different for various orbits, and even worse, it can be positive. (See, for example, the HF calculations quoted in Refs. 6 and 9.) Finally, let us consider one particular example for illustration. The DDHF calculations predict $r=4.893$ and 4.953 fm for ^{87}Sr and ^{93}Nb , respectively. These values correspond to $\partial r/\partial \epsilon$ which is a factor of ~ 2 smaller than the experimental one (irrespective of whether exchange currents are omitted or included). As indicated in Ref. 4, the DDHF fail to accurately reproduce the experimental particle separation energy. When corrected for this failure, the DDHF radii become $r'=4.968$ and 4.973 fm, and $\partial r/\partial \epsilon$ reduces to a value of ~ -0.003 fm MeV $^{-1}$ (as opposed to -0.08 fm MeV $^{-1}$ from experiment). The prediction from DDHFB calculations are $r=4.900$ and 4.862 fm; thus corresponding to a positive value of $\partial r/\partial \epsilon$.

In conclusion, there is evidence from various sources of information that the rms radius of particle orbit within nuclei depends in a simple and regular manner on the particle separation energy. The failure of mean field theories to reproduce such a regularity is a deficiency, more serious perhaps than just being unable to account for several radii of $1f_{7/2}$ and $1g_{9/2}$ nucleon orbits.

Note added in proof. It was brought to my attention by the referee that the exchange current graph involving the delta was not included correctly in Ref. 6. When this term is taken with the proper

sign the exchange current becomes very small.

The author would like to thank Prof. Y. Avishai and Prof. E. Friedman for interesting discussions.

-
- ¹I. Sick, *Comments Nucl. Part. Phys.* **2**, 56 (1980).
- ²S. L. Platchkov, J. B. Bellicard, J. M. Cavedon, B. Frois, D. Goutte, M. Huet, P. Leconte, Phan Xuan Hô, I. Sick, P. K. A. de Witt Huberts, and L. Lapikás, *Phys. Lett.* **86B**, 1 (1979).
- ³P. K. A. de Witt Huberts, L. Lapikás, H. de Vries, J. B. Bellicard, J. M. Cavedon, B. Frois, M. Huet, Ph. Leconte, A. Nakada, Phan Xuan Ho, S. K. Platchkov, and I. Sick, *Phys. Lett.* **71B**, 317 (1977).
- ⁴I. Sick, J. B. Bellicard, J. M. Cavedon, B. Frois, M. Huet, P. Leconte, A. Nakada, Phan Xuan Hô, S. Platchkov, P. K. A. de Witt Huberts, and L. Lapikás, *Phys. Rev. Lett.* **38**, 1259 (1977).
- ⁵P. K. A. de Witt Huberts, J. B. Bellicard, B. Frois, M. Huet, Ph. Leconte, A. Nakada, Phan Xuan Hô, S. Turck, L. Lapikás, H. de Vries, and I. Sick, *Phys. Lett.* **60B**, 157 (1976).
- ⁶J. Dubach, *Nucl. Phys.* **A340**, 271 (1980).
- ⁷P. Woods, R. Chapman, J. L. Durell, J. N. Mo, S. Sen, and A. I. Warwick, *Nucl. Phys.* **A363**, 322 (1981), and references therein.
- ⁸A. Warwick, R. Chapman, J. L. Durell, J. N. Mo, J. A. Kuehner, and P. Skensved, *Nucl. Phys.* **A356**, 33 (1981).
- ⁹A. Warwick, R. Chapman, J. L. Durell, and J. N. Mo, *Phys. Lett.* **87B**, 335 (1979).
- ¹⁰R. Chapman, M. Hyland, J. L. Durell, J. N. Mo, M. Macphail, H. Sharma, and N. H. Merrill, *Nucl. Phys.* **A316**, 40 (1979).
- ¹¹A. Moalem, *Proceedings of the Karlsruhe International Discussion Meeting, Kernforschungszentrum Karlsruhe Report KFK 2830, 1979*, p. 318.
- ¹²A. Moalem, H. T. Fortune, and G. Stephans, *Nucl. Phys.* **A378**, 251 (1982).
- ¹³A. Moalem, *Nucl. Phys.* **A289**, 45 (1977).
- ¹⁴A. Moalem and E. Friedman, *Phys. Rev. Lett.* **40**, 1064 (1978).
- ¹⁵A. Moalem and Z. Vardi, *Nucl. Phys.* **A332**, 195 (1979).
- ¹⁶A. Moalem (unpublished).
- ¹⁷J. W. Negele, L. Zamick, and G. K. Varma, *Comments Nucl. Part. Phys.* **8**, 135 (1979), and references therein.
- ¹⁸J. Mougey, M. Bernheim, A. Bussière, A. Gillebert, Phan Xuan Hô, M. Priou, D. Royer, I. Sick, and G. J. Wagner, *Nucl. Phys.* **A262**, 461 (1976).